Inorganic Chemistry

Article

pubs.acs.org/IC

Mechanistic Details for Cobalt Catalyzed Photochemical Hydrogen Production in Aqueous Solution: Efficiencies of the Photochemical and Non-Photochemical Steps

Bing Shan,[†] Teera Baine,[‡] Xuan Anh N. Ma,[‡] Xuan Zhao,[‡] and Russell H. Schmehl[†,*]

[†]Department of Chemistry, Tulane University, New Orleans, Louisiana 70118, United States
[‡]Department of Chemistry, University of Memphis, Memphis, Tennessee, United States

Supporting Information

ABSTRACT: A detailed examination of each step of the reaction sequence in the photochemical sacrificial hydrogen generation system consisting of $[Ru(bpy)_3]^{2+}$/ascorbate/$[Co(DPA\text{-}bpy)OH_2]^{3+}$ was conducted. By clearly defining quenching, charge separation, and back electron transfer in the $[Ru(bpy)_3]^{2+}$/ascorbate system, the details necessary for evaluation of the efficiency of water reduction with various catalysts are provided. In the particular Co(III) catalyst investigated, it is clear that the light induced catalytic process is considerably less efficient than the electrocatalytic process. A potential source of catalyst inefficiency in this system is reduction of the products formed in oxidation of the sacrificial electron donor. The data provided for excited state quenching and charge separation in this particular aqueous system are meant to be used by others for thorough investigation of the quantum efficiencies of other aqueous homogeneous and nanoheterogeneous catalysts for water reduction.

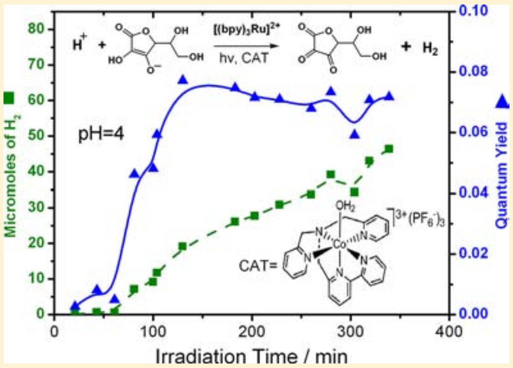

INTRODUCTION

There is growing interest in the development of photochemical systems for the reduction of water to hydrogen and the associated evaluation of both homogeneous and heterogeneous catalysts for water reduction.[1−10] Much of the work on development of catalysts focuses on evaluation of turnover numbers and turnover frequencies in systems involving a variety of chromophores and one of a limited number of sacrificial electron donors.[11−13] While many of the very early investigations reported quantum yields for hydrogen production in addition to turnover information, the barrage of activity to find new, highly active catalysts has resulted in only sporadic publications reporting overall quantum yields, and it is only very recently that research efforts have once again begun to focus on the independent processes contributing to water reduction.[14−16] Among systems reporting quantum yield measurements, the values for net hydrogen generation vary from $<10^{-3}$ to 0.2.[6,17−19] A striking feature is that, despite the fact that the photochemical systems are optimized for reduction and a sacrificial electron donor is used, thereby supposedly eliminating competition from alternative processes for oxidation of the photogenerated reducing agent, the overall hydrogen production quantum yields are often quite low.

A general scheme for a sacrificial three component photochemical water reduction system is shown in Scheme 1. There are several processes that occur sequentially in most sacrificial water reduction systems and some of the steps represent a potential for loss of efficiency; the loss steps are not represented in the scheme. The set of reactions for a general three component system is stated below where C is the chromophore, D is a sacrificial electron donor, Q is a reducible impurity, and Cat, Cat^-, and Cat^{2-} represent the unreduced, singly reduced, and doubly reduced forms of the water reduction catalyst. The widely used $[Ru(bpy)_3]^{2+}$/ ascorbate system[20] (bpy = 2,2′-bipyridine) follows this scheme. The reactions are divided into reducing equivalent generation and hydrogen production.

Scheme 1

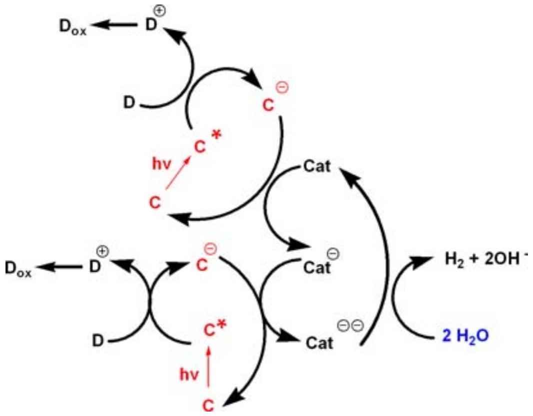

Received: October 31, 2012
Published: April 17, 2013

Reducing Equivalent Generation

$$C + h\nu \rightarrow C^* \tag{1}$$

$$C^* \rightarrow C + h\nu' + \Delta \quad k_r + k_n \tag{2}$$

$$C^* + D \rightarrow \{C^-, D^+\} \quad k_q \tag{3}$$

$$\{C^-, D^+\} \leftrightharpoons C^- + D^+ \quad k_{sep}, k_{-sep} \tag{4}$$

$$\{C^-, D^+\} \rightarrow C + D \quad k_{rec} \tag{5}$$

Catalyst Reduction and Hydrogen Generation

$$C^- + Q \rightarrow C + Q_{red} \quad k_{im} \tag{6}$$

$$C^- + Cat \rightarrow C + Cat^- \quad k_{red1} \tag{7}$$

$$Cat^- + Q' \rightarrow Cat + Q'_{red} \quad k_{icat1} \tag{8}$$

$$C^- + Cat^- \rightarrow C + Cat^{2-} \quad k_{red2} \tag{9}$$

$$Cat^{2-} + Q' \rightarrow Cat + Q'_{red} \quad k_{icat2} \tag{10}$$

$$Cat^{2-} + 2H^+ \rightarrow Cat + H_2 \quad k_{H2} \tag{11}$$

These reactions can be separated into five key elements, and each has an associated efficiency, η: light absorption (F = fraction of incident photons absorbed; eq 1), quenching ($\eta_q = k_q[D]/(k_r + k_n + k_q[D])$; eqs 2,3), charge separation ($\eta_{sep} = k_{sep}/(k_{sep} + k_{rec})$, eqs 4,5), catalyst reduction ($\eta_{red} = k_{red1}[Cat]/(k_{im}[Q] + k_{red1}[Cat]) \sim k_{red2}[Cat^-]/(k_{im}[Q] + k_{red2}[Cat^-])$, eqs 6−10), and hydrogen generation ($\eta_H = k_{H2}\,[H^+]^2/(k_{H2}[H^+]^2 + k_{icat2}[Q'])$, eq 10,11). In this simplified set of reactions, the catalyst reduction efficiency (η_{red}) refers to the average yield for the process of reducing the active forms of the catalyst present in solution during hydrogen evolution; this almost certainly differs from the efficiency for reducing the initial catalytic species introduced. The hydrogen generation reaction represented by eq 11 encompasses all the processes that occur, subsequent to delivery of a second electron to the catalyst, that lead to hydrogen formation. Nonproductive side reactions of the reduced chromophore, C^-, and the reduced catalyst, Cat^{2-}, are represented by reactions 6, 8, and 10. The overall efficiency of hydrogen generation can then be stated as the product of the efficiencies for generating Cat^- ($\eta_{cat\text{-}cat1}$), Cat^{2-} ($\eta_{cat1\text{-}cat2}$), and H_2 from Cat^{2-} ($\eta_{cat2\text{-}H2}$). Assuming the efficiencies for the reaction of C^- with Cat and Cat^- are nearly the same, the hydrogen formation quantum yield can be expressed as

$$\begin{aligned}\Phi_{H2} &= 0.5(\eta_{cat-cat1}\eta_{cat1-cat2}\eta_{cat2-H2}) \\ &\sim 0.5[F(\eta_q)(\eta_{sep})(\eta_{red})]^2(\eta_H)\end{aligned} \tag{12}$$

Since the measured quantum yield is stated as moles of H_2 produced per quanta of photons incident on the system, the limiting values for η_H and Φ_{H2} are 0.5.[14] The above description is a simplified general description of reaction of the doubly reduced catalyst with protons to yield hydrogen and ignores the mechanistic details of catalyst reaction with protons and the possibility of disproportionation of the singly reduced catalyst. Also neglected is the possible recombination of solvent separated C^- and D^+ (k_{-sep}) since C^- will very likely be rapidly consumed by Cat or Cat^- under pseudo-first-order conditions (*vide infra*).

The fraction of light absorbed, F, can be readily controlled to be nearly unity, especially when irradiation is restricted to a band of light around the absorption maximum of the chromophore. In addition, the quenching efficiency is limited only by the solubility of the quencher and the quenching rate constant. Escape of the radical ions from the geminate pair formed in the electron transfer quenching event is often significantly less than unity (for $[Ru(bpy)_3]^{2+}$ and methyl viologen, the charge separation yield following oxidative electron transfer is only 0.25[21]). Charge separation yields can be strongly dependent on temperature and, to a lesser extent, on ionic strength.[22,23] This is one of the key pieces of information lacking for many photochemical reduction systems. However, perhaps the most important processes to evaluate in photochemical water reduction systems are the outersphere catalyst reduction (and reduction of partially reduced/intermediate catalytic species) by the reduced chromophore (eqs 7 and 9; rate and overall efficiency of reduction) and the hydrogen production efficiency of the reduced, active catalyst, η_H.

The work of others has focused on one or more of these elements, but there have only been a few systems for which all of these aspects of the hydrogen generation are considered collectively to evaluate the sources of loss of efficiency. There are two recent papers that present many of the above details. In a 2011, paper by Fukuzumi and co-workers evaluating a system consisting of $[Ru(bpy)_3]^{2+}$ as a chromophore, ascorbate as the sacrificial electron donor, and a Rh (or Ir) homogeneous catalyst for water reduction,[14] they discuss some of these mechanistic aspects in detail and also provide hydrogen yields for the overall process. A separate effort by Hamm and Alberto discusses a system involving a rhenium diimine complex chromophore, ascorbate donor, and a cobalt imine water reduction catalyst; their work clearly indicates quenching rate constants, the charge separation yield for the reduced Re complex/oxidized ascorbate cage, and the rate constant for the bimolecular reaction of the reduced Re complex and the divalent cobalt water reduction catalyst.[1,24] From each of these papers, the sources of loss can be quantitatively evaluated, and the effectiveness of the catalyst can be extracted (*vide infra*). In this work, we have examined the $[Ru(bpy)_3]^{2+}$ chromophore/ascorbate ion quencher system in combination with a Co(III) catalyst, $[Co(DPA\text{-}bpy)OH_2]^{3+}$ (DPA-bpy = N,N-bis(2-pyridinylmethyl)-2,2′-bipyridine-6-methanamine, Figure 1), recently reported by Zhao and co-workers.[6] They found that hydrogen production in buffered aqueous solutions is most efficient at pH 4. Here, we examine the system in detail, dissecting each of the contributing reactions and evaluating the sources of loss in the system and the overall effectiveness of the catalyst under different solution conditions. A simple actinometric procedure is given to aid others in determining quantum

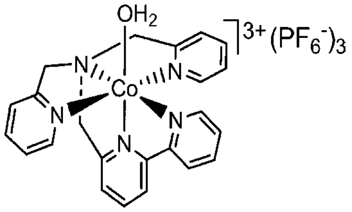

Figure 1. Cobalt(III) catalyst used for reduction of water.

yields for hydrogen production in aqueous solutions using this system.

EXPERIMENTAL SECTION

$[Ru(bpy)_3]Cl_2$ was prepared according to a published procedure,[25] although it is available commercially from several sources. Sodium ascorbate (Sigma-Aldrich), sodium acetate (Fisher), and acetic acid (Fisher) were used without further purification. The cobalt catalyst, $[Co(DPA\text{-}bpy)OH_2](PF_6)_3$, was prepared based on a literature method.[6]

Luminescence Quenching. The quenching of $[Ru(bpy)_3]^{2+}$ luminescence by ascorbate was examined in buffered aqueous solutions at several solution acidities over the pH range 3 to 7. The chromophore and ascorbate quencher solutions were prepared from a 0.1 M stock acetate/acetic acid buffer solution. Stern−Volmer luminescence quenching measurements were carried out in aerated solutions using a PTI Felix 32 MD-5020 spectrofluorimeter.

Transient Absorption and Luminescence Lifetime Measurements. Transient absorption spectra were obtained using an Applied Photophysics LKS 60 optical system with pulsed excitation by an OPOTEK visible OPO that was pumped by a Quantel Brilliant Laser equipped with doubling and tripling crystals. Excitation of the chromophore was typically at 460 nm using samples having an optical density of between 0.6 and 0.8. Luminescence lifetimes were obtained for both aerated and nitrogen degassed samples by averaging decays of emission at 610 nm.

Charge Separation Measurements. Charge separation yields were determined by using the $[Ru(bpy)_3]^{2+}$ excited state absorption at 360 nm (ε = 18 000 M^{-1} cm^{-1})[26] to obtain the concentration of excited states formed. The concentration of ions escaping the geminate pair was determined from the 510 nm[27−30] absorbance of the $[Ru(bpy)_3]^+$ (ε = 12 000 M^{-1} cm^{-1})[31] obtained following the laser pulse. With these two values and the fraction of excited states quenched by the ascorbate, η_q, the charge separation yield can be determined as

$$\eta_{cs} = (\Delta A_{510}\Delta\varepsilon_{360})/(\Delta A_{360}\Delta\varepsilon_{510}\eta_q)$$

H_2 Production Quantum Yields. The output of a 150 W Xe arc lamp, fitted with optical filters to provide a bandpass between 420 and 520 nm (Schott GG420 and UG1), was passed through a 5 cm path of water and focused into a 1 cm^2 spectrophotometric cell. The irradiation spot size at the cell surface was approximately 1 cm in diameter. Lamp actinometry was carried out using the photooxidation of $[Ru(bpy)_3]^{2+}$ by $S_2O_8^{2-}$ (protocol in Supporting Information). Samples (3.5 mL volume) containing the Ru(II) complex (Abs = 1.5 at 450 nm), sodium ascorbate (0.4 M), acetic acid buffer (0.1 M), and the cobalt catalyst (5 μM) were degassed by bubbling with nitrogen and sealed with a screwcap having a rubber septum (cells from Spectrocell). The headspace volume was 1.3 mL. After irradiation for variable periods of time, a 150 μL sample of gas was extracted and injected into a gas chromatograph (Gow-Mac GC; Molecular Sieve Column, T = 35 °C; carrier gas: N_2) for quantitative determination of the volume of H_2 produced. The quantum yield for hydrogen production per absorbed photon is determined from

$$\Phi_{H2} = \frac{\text{moles } H_2 \text{ produced}}{\text{moles photons absorbed}} = \left(\frac{V}{RT}\right)\left(\frac{1}{ItF}\right)$$

where V_{H2} is the volume of hydrogen produced in the cell headspace as determined by gas chromatography, R is the gas constant, T is the temperature, I is the lamp intensity (quanta/s, from actinometry), F is the fraction of photons absorbed, and t is the irradiation time.[19,32−37] An alternative approach is to measure pressure changes in the cell as a function of irradiation time, assuming ideal gas behavior for the hydrogen.

In the irradiations carried out in this work, the amount of dissolved hydrogen was 2% or less in all cases. Using a Henry's law constant of 7.8×10^{-4} M/atm for hydrogen,[38] the number of moles of dissolved hydrogen is 7.6×10^{-7} when the partial pressure of hydrogen in the gas phase is 0.28 atm, which corresponds to 40 μmol of hydrogen in the gas phase in the photolysis system used.

RESULTS AND DISCUSSION

Excited State Quenching. Rate constants for quenching of $[Ru(bpy)_3]^{2+}$ by ascorbate have been reported in earlier publications.[2,6,14,20,33,39] In the majority of earlier work, what one finds is a series of references that ultimately refer back to a single report by Creutz et al. in 1979 (at pH 4 $k_q = 2 \times 10^7$ M^{-1} s^{-1}).[40] Since there has been a revival in the use of this chromophore−quencher combination as a sacrificial system for hydrogen generation, we have examined the quenching process over a range of pH (acetate buffer); values are reported in Table 1. Ascorbic acid (H_2A) has two measurable dissociation constants at room temperature with pK values of 4.1 and 11.8. Thus, the predominant form of the quencher at pH 3 will be the fully protonated acid (HA^-, ~8%). At pH 4, which turns out to be optimal for H_2 production with the cobalt catalyst examined in this work, the concentrations of H_2A and HA^- are nearly equal, and at higher pH, the anion is the predominant species.[41] It is perhaps a bit surprising that the quenching rate constants vary by only a factor of 2 over the entire range, but the rate constant is approximately a factor of 1000 slower than the diffusion limited rate constant and certainly slower than proton exchange processes associated with ascorbic acid. For the purposes of hydrogen generation, quenching of a high fraction of the excited states by a dynamic quenching process ($\tau_o/\tau \sim 100$) is not possible. Using 0.5 M ascorbate at pH 4 results in 71% of excited $[Ru(bpy)_3]^{2+}$ (τ_0 = 500 ns) being quenched.

Table 1. Rate Constants and Yields Obtained for Quenching, Charge Separation, and Back Reaction in the $[Ru(bpy)_3]^{2+}$/Ascorbate System in Acetate Buffer Solutions[a]

pH	k_q, × 10^7 M^{-1} cm^{-1} (±15%)	η_q 0.1 M Asc (±0.05)	η_{cs} (±0.15)	k_b, × 10^{10} M^{-1} cm^{-1} (±15%)
2.74	0.89	0.37	0.99	1.1
3.44	0.94	0.38	0.99	1.1
4.04	1.0	0.40	0.77 (0.79)	2.1
4.48	1.0	0.39	0.95	1.8
5.16	1.1	0.42	0.86	2.0
5.93	1.1	0.42	0.92	0.87
6.86	1.2	0.42	0.99	1.3
7.85	1.2	0.44	0.94	0.78

[a] k_q = Rate constant for quenching of the $[Ru(bpy)_3]^{2+}$ luminescence, η_q is the fraction of excited states quenched with 0.1 M ascorbate, η_{cs} is the charge separation efficiency from the geminate pair formed in the quenching event, and k_b is the rate constant for recombination of $[Ru(bpy)_3]^+$ and the ascorbate radical anion.

Cage Escape Yields. A key aspect for any photochemical system involving bimolecular electron transfer is the yield of ions that escape the geminate pair formed in the photoredox reaction. The measurement requires determination of the concentration of excited states formed, the fraction of excited states quenched by the ascorbate ion and the total concentration of reactive ions in solution following the charge separation process. Since $[Ru(bpy)_3]^{2+}$ reacts from a triplet excited state, the intersystem crossing efficiency is also a factor in evaluation of the charge separation yield; a variety of measurements over the past 30 years have led to the conclusion that the intersystem crossing efficiency is unity for this chromophore. The concentration of triplet excited states formed was determined from the absorbance of the ^{3}MLCT state at 360 nm. The absorptivity change ($\Delta\varepsilon$) associated with the $[\mathrm{Ru(bpy)_3}]^{2+}$ has been a point of discussion for many years. Here, we make use of the value obtained by Hoffman and coworkers (18 000 $\mathrm{M^{-1}\ cm^{-1}}$) and supported by the recent results of Brettel;[26] their value was determined by inference from the bleach of the transient absorption at 450 nm.

Excited state electron transfer from the ascorbate to the excited Ru complex results in formation of the ascorbate radical ($\mathrm{HA^{\bullet}}$), which rapidly deprotonates to generate the ascorbate anion radical ($\mathrm{A^{-\bullet}}$)[4] and the one electron reduced Ru complex. The transient spectral changes observed for the $[\mathrm{Ru(bpy)_3}]^{2+}$/ascorbate system at pH 4 are shown in Figure 2. The excited state of the Ru complex has a maximum at 360 nm, as does the $[\mathrm{Ru(bpy)_3}]^{+}$ which is formed as the excited state decays. The reduced Ru complex also has a unique absorption maximum at 510 nm. The concentration of $[\mathrm{Ru(bpy)_3}]^{+}$ formed following cage escape was determined from the 510 nm transient where only the Ru(II) and Ru(I) complexes absorb.[42] The cage escape yields, determined from the concentration of excited states formed, the fraction of excited states quenched, and the concentration of reduced Ru complex in solution immediately following the laser pulse, are listed in Table 1 at each pH studied. Yields at all pH values measured are 0.9 ± 0.15 and are, within the margin of error, independent of pH, although for pH 4, repeated measurements suggest a lower charge separation yield of 0.78 ± 0.10. Charge separation yields determined for a variety of electron donors and acceptors involved in quenching of $[\mathrm{Ru(bpy)_3}]^{2+}$ have been determined, and yields for the formation of radical ions following reduction of the Ru chromophore are generally quite high. In most systems for which high yields are obtained, the quencher is a neutral electron donor, so the encounter complex goes from a dication/neutral to a pair of monocations. In this system, the geminate ion pair involves a dication/anion encounter complex that evolves to a monocation/neutral. Whether deprotonation of the neutral radical occurs within the encounter complex is not known. Ionic strength has been shown to play a role in charge separation, and independent studies by Hoffman et al. and Harriman et al. illustrate the quantitative dependence of ionic strength on charge separation yields in systems involving pentacation/monocation and trication/monocation geminate pairs.[22,23] In this case, the geminate pair involves a cation and a neutral, and Coulombic effects of solvent ionic strength variations are likely to be significantly less important. We examined the ionic strength dependence in solutions having relatively high total ion concentration (>0.6 M, required because of the large concentration of ascorbate needed to quench a significant fraction of the excited states formed) and found no discernible variation in the charge separation yield (see Supporting Information).

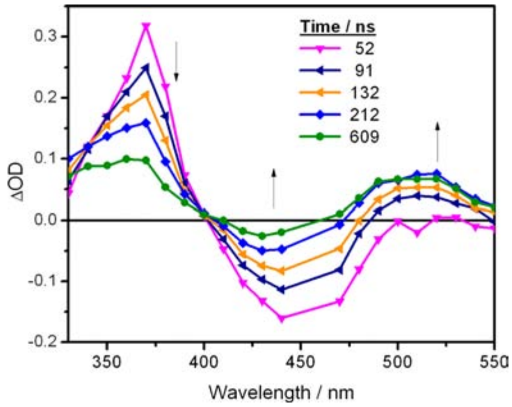

Figure 2. The transient spectral changes observed for the $[\mathrm{Ru(bpy)_3}]^{2+}$/ascorbate system in water at pH 4 with an ascorbate concentration of 0.4 M.

Back Electron Transfer and Catalyst Reduction. In the absence of a cobalt catalyst, the reduced ruthenium complex undergos back electron transfer with the oxidized ascorbate ion (which is an anion). Previous work has thoroughly documented the acid–base chemistry of one electron oxidized ascorbate,[4] and at pH 4 and above, the initially formed ascorbate radical deprotonates to produce an anion radical (eq 13)[41]

$$\mathrm{HA^{\bullet}} \leftrightharpoons \mathrm{A^{-}} + \mathrm{H^{+}} \quad \mathrm{p}K = -0.86 \qquad (13)$$

Figure 3 shows the decay of the absorbance of the $[\mathrm{Ru(bpy)_3}]^{+}$ transient at 510 nm following quenching and charge separation with the ascorbate ion at pH 6.9. The fact that back electron transfer occurs indicates that ascorbate is not a typical sacrificial electron donating quencher. The rate constant for the back electron transfer reaction is near the diffusion limit over the entire pH range, and no net spectral changes are observed in flash photolysis experiments. Thus, reduction of the catalyst by the $[\mathrm{Ru(bpy)_3}]^{+}$ must compete with back electron transfer.

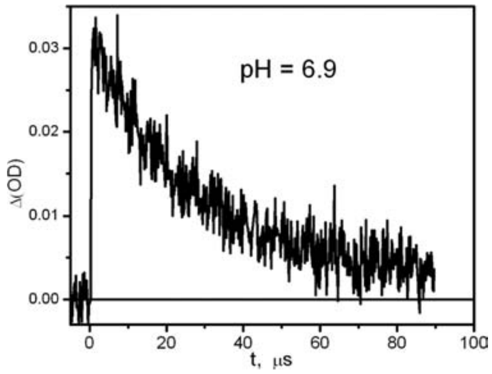

Figure 3. The decay of the absorbance of the $[\mathrm{Ru(bpy)_3}]^{+}$ transient at 510 nm following quenching and charge separation with 0.1 M ascorbate ion at pH 6.9.

Figure 4 illustrates changes in the absorbance of reduced Ru at 510 nm in solutions with and without added cobalt catalyst (325 μM). Since concentrations of $[\mathrm{Ru(bpy)_3}]^{+}$ formed are in the micromolar concentration range, the reaction of the reduced Ru with the Co(III) complex follows pesudo-first-order kinetics, and with the given concentration of Co(III) in solution, the catalyst reduction competes effectively with back electron transfer. At pH 4, the second order rate constant obtained for reduction of the Co(III) by Ru(I) (eq 7) is $5 \times 10^9\ \mathrm{M^{-1}\ s^{-1}}$. Figure 4 also shows the decay of the $[\mathrm{Ru(bpy)_3}]^{+}$ in the presence of the Co(II) form of the catalyst. The rate constant obtained is within experimental error of that for reduction of the Co(III) catalyst. The reaction with Co(II) was carried out in two ways: using a sample of the Co(II) complex independently prepared in the Zhao laboratory and using Co(II) generated *in situ* by Zn reduction. Repeated experiments consistently yielded the same kinetic result. The rate constant obtained, $5 \times 10^9\ \mathrm{M^{-1}\ s^{-1}}$, is near the diffusion limit. Given that the $[\mathrm{Ru(bpy)_3}]^{+}$ is a 1.2 V reductant (vs SHE) and the reported

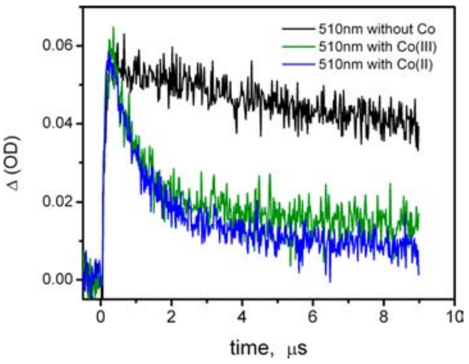

Figure 4. Transient absorbance changes at 510 nm following excitation of Ru, ascorbate (0.4 M), and Co(III) (325 μM, green decay) or Co(II) (315 μM, blue decay).

potentials for the sequential cobalt catalyst reduction are < −1.0 V vs SHE (Co(III/II) = 0.15 V; Co(II/I)= −0.9 V/quasi-reversible),[6] it is certainly possible that the reduction reactions could both be near the diffusion limit.

It is important to note that, under conditions for hydrogen production, concentrations of the cobalt catalyst used are 40 μM or less, and it might be envisioned that back electron transfer with the ascorbate anion (eq 14) would compete effectively with catalyst reduction.

$$[\text{Ru(bpy)}_3]^+ + \text{Asc}^{\dot{-}} + \text{H}^+ \rightarrow [\text{Ru(bpy)}_3]^{2+} + \text{HAsc}^- \quad k_b \tag{14}$$

However, steady state photocatalytic conditions involve much lower light intensities than those used in laser flash photolysis, and the steady state concentration of both reduced ruthenium and the ascorbate anion will be orders of magnitude lower. For example, at typical AM1 solar intensities of 100 mW cm^{-2} being completely absorbed within a depth of 1 cm (volume = 1 cm^3), a very simple estimate of the flux of photons, making the simplification that all photons are 500 nm, gives 0.4 mM photons per second impinging on the sample. Assuming that every photon results in formation of a radical ion (not true in this system) and that the rate of production of radical ions equals the rate of disappearance through only back electron transfer, it is appropriate to state (eq 15) that

$$\begin{aligned} 0.4\ \text{mM photons/s} &= -d[\text{Ru(I)}]/dt \\ &= k_b[\text{Ru(I)}][\text{Asc}^{\dot{-}}] = k_b[\text{Asc}^{\dot{-}}]^2 \end{aligned} \tag{15}$$

and therefore, the steady state concentration of both reduced Ru and ascorbate under these conditions would be 0.2 μM, more than an order of magnitude lower than the concentration of the cobalt catalyst used. Assuming that the only pathways for reaction of the [Ru(I)] formed are reaction with the cobalt catalyst or back reaction with the ascorbate radical anion present, and given the rate constants determined (Table 1), a [Co(III)] concentration of 5 μM, and the above estimated concentration of radical ions present (which is an over-estimate), the approximate efficiency for reduction of cobalt would be over 90%.

$$\eta_{\text{red}} = \text{k}_{\text{red}}[\text{Co(III)}]/(k_b[\text{Asc}^-] + k_{\text{red}}[\text{Co(III)}]) = 0.93$$

It is interesting to note that use of solar concentration in a steady state photolysis of this sort could actually serve to decrease the efficiency of catalyst reduction because the steady state concentration of $[\text{Ru(bpy)}_3]^+$ and the ascorbate radical ion would increase, thereby allowing the back reaction to compete with reduction of the cobalt catalyst.

Hydrogen Production Yields. Since the intensity of the irradiation source and the concentration of the catalyst directly impact the efficiency of catalyst reduction, the purpose for determination of hydrogen formation yields is to account for the other independent factors that serve to limit the hydrogen production efficiency: the fraction of light absorbed, the fraction of excited states quenched, and the charge separation efficiency.

The measurement requires determination of the rate of photons entering the photolysis cell and also requires the fraction of photons absorbed to be determined. In our system, the output of a Xe arc lamp, equipped with appropriate bandpass filters, was focused into the center of a standard spectrophotometric cuvette holder, and lamp intensity measurements were performed by irradiating the actinometer in this configuration. This system is representative of a typical commercial spectrofluorimeter, excepting the fact that a monochromator would be used to set the irradiation bandpass. Actinometry was carried out using an aqueous solution of $[\text{Ru(bpy)}_3]^{2+}$ containing potassium persulfate that irreversibly oxidizes the Ru(II) upon photolysis;[43−45] the protocol is given in the Supporting Information.

Hydrogen production was determined by two methods: direct measurement of evolved hydrogen using gas chromatography and measurement of pressure changes in the cell during photolysis. Figure 5 shows the amount of hydrogen produced in the photolysis at pH 4 with 5 μM catalyst as a function of time in a typical run as measured by gas chromatography. The quantum yield, calculated as the photolysis proceeded, is also shown. For the cobalt catalyst employed, there is an incubation time during which the catalyst is reduced from the initial [Co(III)] species to the catalytically reactive form, presumably formally a [Co(I)] complex. We have not been able to observe the reduced cobalt species directly via UV−visible laser flash photolysis and thus we cannot follow the reaction of the reduced cobalt species with protons (and subsequent reactions leading to hydrogen formation). After approximately 2 h irradiation time, the quantum yield reaches a plateau, indicating the system has reached a steady state; the hydrogen produced continues to increase as the system remains functional. Ultimately, when the system no longer produces hydrogen, the measured overall quantum yield will decline with continued

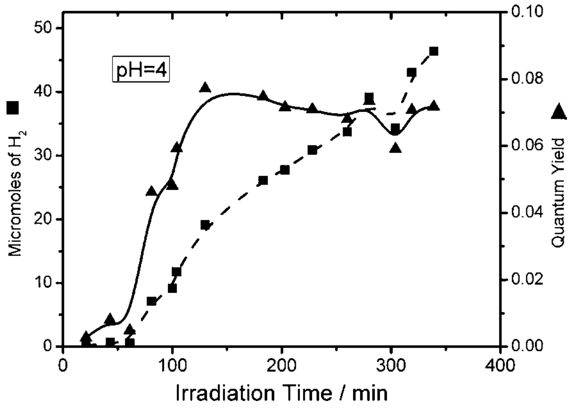

Figure 5. The amount of hydrogen produced and quantum yield of H_2 formation in the photolysis at pH 4 with 5 μM catalyst as a function of time in a typical run for hydrogen measured by GC.

irradiation time. In all systems studied, the irradiation was discontinued before the system ceased to produce hydrogen.

From the result of Φ_{H2} of 0.07 (on average) at pH 4, with the fraction of light absorbed being 1.0, the fraction of excited states quenched at 0.7, a charge separation efficiency of 0.78, and the fraction of catalyst reduced assumed to be 1.0, the efficiency for H_2 production is 0.23; the limiting yield is 0.5. So effectively the efficiency for reaction of the doubly reduced catalyst with water to produce hydrogen is 46%.

Quantum yields for generation of hydrogen were also determined at various pH levels and at two different catalyst concentrations. Figure 6 illustrates the quantum yield measured as a function of irradiation time for the varying experimental conditions. The hydrogen yield is lower at both higher and lower pH (Figure 6A). This agrees with observations made by others using $[Ru(bpy)_3]^{2+}$ as a sensitizer and ascorbate as a donor in hydrogen generation systems with other catalysts.[1,14,24,46] The data in Table 1 clearly show that the significant decrease in the hydrogen generation quantum yield at pH 5 is not related to the fraction of excited states quenched, the charge separation efficiency, or back electron transfer and is therefore related to a pH dependent aspect of the cobalt catalyst. All mechanistic routes postulated for these systems involve protonation of the cobalt catalyst, and it is likely that pH 5 is above the p*K* for the reduced form of the cobalt catalyst that undergoes protonation. Interestingly, increasing the cobalt catalyst concentration from 5 μM to 40 μM results in a significant decrease in the quantum yield for hydrogen formation (Figure 6B). From the point of view of trapping the reducing agent, $[Ru(bpy)_3]^+$, higher catalyst concentrations are obviously beneficial, so the loss in hydrogen production efficiency must result from losses in subsequent steps of the process.

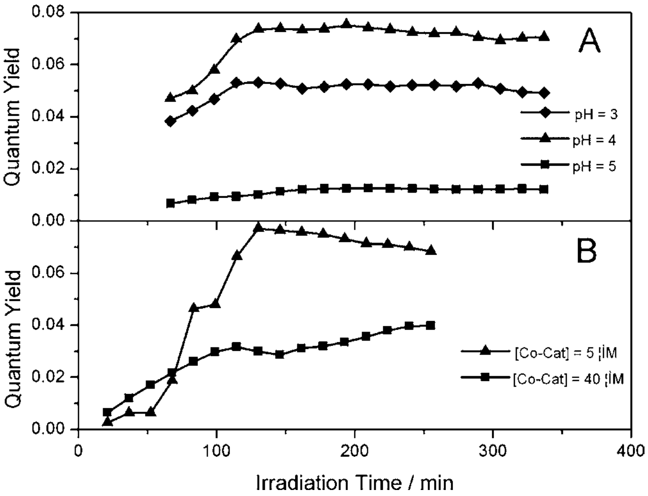

Figure 6. Measured hydrogen production quantum yields as a function of pH (A) for pH 3, 4, and 5 and at Co(III) catalyst concentrations of 5 μM and 40 μM.

The relatively low yield for catalyst activity, approximately 46% of the potential yield at pH 4, is interesting when one considers the faradaic efficiency measured for the catalyst in electrochemical experiments (~ 0.98 at pH 7 phosphate buffer).[6] While the measurements are made under considerably different conditions, it should be noted that quantum yield measurements for the photochemical route to hydrogen production decrease further upon increasing the pH toward that used in the electrochemical experiments. The decrease in hydrogen yield with increasing pH has been observed for $[Ru(bpy)_3]^{2+}$/ascorbate systems with other catalysts for hydrogen generation, which suggests that the pH dependence may arise from a reaction preceding the reduction of the catalyst. However, results of Table 1 indicate only small changes in the quenching rate constant, charge separation yield, and back electron transfer rates with pH, suggesting the decrease in efficiency with increasing pH lies with the catalyst. Electrochemical reduction maintains a fixed overpotential, and the environment near the electrode surface is necessarily strongly reducing during the entire process. In addition, no other reactants (other than water and buffer) are present in solution. The "sacrificial" photochemical system is quite different. In comparison to electrochemical reduction, the flux of reducing equivalents in the photochemical system is significantly lower. Given the lamp intensity and relative efficiencies of charge separation and electron transport, the flux of reducing electrons (from photons cm^{-2} s^{-1} incident on the photolysis cell) is less than 1/50 that of typical electrochemical experiments.[6] As a result, the half-lives of intermediate forms of the reduced Co complex are likely to be significantly longer in the photochemical experiment, providing opportunities for reduction of other species in solution. In addition, the photolysis solution contains oxidized forms of ascorbic acid, including dehydroascorbic acid and its hydrolysis product, that accumulate during the photoreduction process. We have not explored rate constants for reduction of these species by either Co(I) species or possibly even Co(II) species, but the reactions are almost certainly thermodynamically favorable and may well be kinetically competitive with the hydrogen generation reaction under these pseudo-first-order conditions where high concentrations of the oxidized form of the sacrificial donor exist.

■ SUMMARY

In this work, we have investigated in detail the losses in efficiency in a widely studied sacrificial photochemical system for water reduction. By clearly defining quenching, charge separation, and back electron transfer in the $[Ru(bpy)_3]^{2+}$/ascorbate system, the details necessary for evaluation of the efficiency of water reduction catalysts have been provided. In the particular Co(III) catalyst investigated, it is clear that the light induced catalytic process is considerably less efficient than the electrocatalytic process. A potential source of catalyst inefficiency in this system is reduction of the products formed in oxidation of the sacrificial electron donor. The data provided for excited state quenching and charge separation allow for facile investigation of the quantum efficiencies of other aqueous homogeneous and nanoheterogeneous catalysts for water reduction.

■ ASSOCIATED CONTENT

Ⓢ Supporting Information

Actinometry for quantum yields. This material is available free of charge via the Internet at http://pubs.acs.org.

■ AUTHOR INFORMATION

Corresponding Author

*E-mail: russ@tulane.edu.

Notes

The authors declare no competing financial interest.

■ ACKNOWLEDGMENTS

R.H.S. thanks the U.S. Department of Energy, Office of Chemical Sciences (Grant DE-FG-02-96ER14617) for support of this research. X.Z. acknowledges NSF EPS 1004083 for the support of T.B. and X.A.N.M.

■ REFERENCES

(1) Guttentag, M.; Rodenberg, A.; Kopelent, R.; Probst, B. *Eur. J. Inorg. Chem.* **2012**, 59−64.

(2) Sano, Y.; Onoda, A.; Hayashi, T. *Chem Commun.* **2011**, *47*, 8229−8231.

(3) Creutz, C.; Sutin, N.; Brunschwig, B. S. *J. Am. Chem. Soc.* **1979**, *101*, 1297−1298.

(4) Bielski, B. H. J.; Allen, A. O.; Schwarz, H. A. *J. Am. Chem. Soc.* **1981**, *103*, 3516−3518.

(5) Chandrasekaran, K.; Whitten, D. G. *J. Am. Chem. Soc.* **1980**, *102*, 5119−20.

(6) Singh, W. M.; Baine, T.; Kudo, S.; Tian, S.; Ma, X. A. N.; Zhou, H.; DeYonker, N. J.; Pham, T. C.; Bollinger, J. C.; Baker, D. L.; Yan, B.; Webster, C. E.; Zhao, X. *Angew. Chem.* **2012**, *51*, 5941−5944.

(7) Cook, T. R.; Dogutan, D. K.; Reece, S. Y.; Surendranath, Y.; Teets, T. S.; Nocera, D. G. *Chem. Rev.* **2010**, *110*, 6474−502.

(8) Esswein, A. J.; Nocera, D. G. *Chem. Rev. (Washington, DC, U. S.)* **2007**, *107*, 4022−4047.

(9) Teets, T. S.; Nocera, D. G. *Chem. Commun. (Cambridge, U. K.)* **2011**, *47*, 9268−9274.

(10) McCormick, T. M.; Han, Z.; Weinberg, D. J.; Brennessel, W. W.; Holland, P. L.; Eisenberg, R. *Inorg. Chem.* **2011**, *50*, 10660−10666.

(11) Han, Z.; McNamara, W. R.; Eum, M.; Holland, P. L.; Eisenberg, R. *Angew. Chem., Int. Ed.* **2012**, *51*, 1667−1670 , S1667/1−S1667/14.

(12) McLaughlin, M. P.; McCormick, T. M.; Eisenberg, R.; Holland, P. L. *Chem. Commun. (Cambridge, U. K.)* **2011**, *47*, 7989−7991.

(13) Du, P.; Schneider, J.; Luo, G.; Brennessel, W. W.; Eisenberg, R. *Inorg. Chem. (Washington, DC, U. S.)* **2009**, *48*, 4952−4962.

(14) Fukuzumi, S.; Kobayashi, T.; Suenobu, T. *Angew. Chem.* **2011**, *50*, 728−731.

(15) Sabatini, R. P.; McCormick, T. M.; Lazarides, T.; Wilson, K. C.; Eisenberg, R.; McCamant, D. W. *J. Phys. Chem. Lett.* **2011**, *2*, 223−227.

(16) McCormick, T. M.; Calitree, B. D.; Orchard, A.; Kraut, N. D.; Bright, F. V.; Detty, M. R.; Eisenberg, R. J. *Am. Chem. Soc.* **2010**, *132*, 15480−15483.

(17) Gurunathan, K. *Int. J. Hydrogen Energy* **2004**, *29*, 933−940.

(18) Arachchige, S. M.; Brown, J.; Brewer, K. J. *J. Photochem. Photobiol., A* **2008**, *197*, 13−17.

(19) Amouyal, E.; Koffi, P. C. R. *Acad. Sci., Ser. 2* **1985**, *300*, 199−202.

(20) McNamara, W. R.; Han, Z.; Alperin, P. J.; Brennessel, W. W.; Holland, P. L.; Eisenberg, R. *J. Am. Chem. Soc.* **2011**, *133*, 15368−15371.

(21) Chiorboli, C.; Indelli, M. T.; Rampi Scandola, M. A.; Scandola, F. *J. Phys. Chem.* **1988**, *92*, 156−63.

(22) Gore, B. L.; Harriman, A.; Richoux, M. C. *J. Photochem.* **1982**, *19*, 209−214.

(23) Sun, H.; Yoshimura, A.; Hoffman, M. Z. *J. Phys. Chem.* **1994**, *98*, 5058−5064.

(24) Probst, B.; Guttentag, M.; Rodenberg, A.; Hamm, P.; Alberto, R. *Inorg. Chem.* **2011**, *50*, 3404−3412.

(25) Broomhead, J. A.; Young, C. G.; Hood, P. *Inorg. Synth.* **2007**, 338−340.

(26) Murov, S. L.; Hug, G. L.; Carmichael, I. *In Handbook of Photochemistry*; M. Dekker: New York, 1993; pp 420.

(27) Balzani, V.; Bolletta, F.; Scandola, F.; Ballardini, R. *Pure Appl. Chem.* **1979**, *51*, 299−311.

(28) Balzani, V.; Moggi, L.; Manfrin, M. F.; Bolletta, F.; Gleria, M. *Science* **1975**, *189*, 852−6.

(29) Garcia, H.; Lopez-Nieto, J. M.; Palomares, E.; Roth, H. D.; Solsona, B. *J. Mater. Chem.* **2006**, *16*, 216−220.

(30) Giansante, C.; Ceroni, P.; Balzani, V.; Vogtle, F. *Angew. Chem., Int. Ed.* **2008**, *47*, 5422−5425.

(31) Miedlar, K.; Das, P. K. *J. Am. Chem. Soc.* **1982**, 7462−7469.

(32) Amouyal, E.; Koffi, P. *J. Photochem.* **1985**, *29*, 227−42.

(33) Brown, G. M.; Brunschwig, B. S.; Creutz, C.; Endicott, J. F.; Sutin, N. *J. Am. Chem. Soc.* **1979**, *101*, 1298−300.

(34) Brown, G. M.; Chan, S. F.; Creutz, C.; Schwarz, H. A.; Sutin, N. *J. Am. Chem. Soc.* **1979**, *101*, 7638−40.

(35) Brunschwig, B. S.; Sutin, N. *Chem. Phys. Lett.* **1981**, *77*, 63−5.

(36) Caspar, J. V.; Meyer, T. J. *J. Am. Chem. Soc.* **1983**, *105*, 5583−90.

(37) Crosby, G. A.; Demas, J. N.; Callis, J. B. *J. Res. Nat. Bur. Stand., Sect. A* **1972**, *76*, 561−77.

(38) Sander, R. *Compilation of Henry's Law Constants for Inorganic and Organic Species of Potential Importance in Environmental Chemistry*. http://www.henrys-law.org/henry.pdf (accessed 01/22, 2013).

(39) Creutz, C.; Schwarz, H. A.; Sutin, N. *J. Am. Chem. Soc.* **1984**, *106*, 3036−7.

(40) Creutz, C.; Sutin, N.; Brunschwig, B. *J. Am. Chem. Soc.* **1979**, *101*, 1298−1300.

(41) Bielski, B. H. J.; Comstock, D. A.; Bowen, R. A. *J. Am. Chem. Soc.* **1971**, *93*, 5624−5629.

(42) Kelly, L. A.; Rodgers, M. A. J. *J. Phys. Chem.* **1994**, *98*, 6377−6385.

(43) Kaledin, A. L.; Huang, Z.; Geletii, Y. V.; Lian, T.; Hill, C. L.; Musaev, D. G. *J. Phys. Chem. A* **2010**, *114*, 73−80.

(44) Montalti, M.; Credi, A.; Prodi, L.; Gandolfi, M. T. In *Handbook of Photochemistry*, 3rd ed.; Taylor and Francis: Boca Raton, FL, 2006; pp 635.

(45) Njapba, N. J.; Waltz, W. L. *Afr. J. Sci. Technol.* **2001**, *2*, 12−16.

(46) Wang, F.; Wang, W.; Wang, X.; Wang, H.; Tung, C.; Wu, L. *Angew. Chem., Int. Ed.* **2011**, *50*, 3193−3197.